IEEE Access
Multidisciplinary | Rapid Review | Open Access Journal

Received January 4, 2019, accepted January 29, 2019, date of publication February 1, 2019, date of current version March 8, 2019.

Digital Object Identifier 10.1109/ACCESS.2019.2896918

Seam Manipulator: Leveraging Pixel Fusion for Depth-Adjustable Stereoscopic Image Retargeting

XIONGLI CHAI[1], FENG SHAO[1], (Member, IEEE), QIUPING JIANG[1], (Student Member, IEEE), AND YO-SUNG HO[2], (Fellow, IEEE)

[1]Faculty of Information Science and Engineering, Ningbo University, Ningbo 315211, China
[2]School of Information and Communications, Gwangju Institute of Science and Technology, Gwangju 500-712, South Korea

Corresponding author: Feng Shao (shaofeng@nbu.edu.cn)

This work was supported in part by the Natural Science Foundation of China under Grant 61622109, in part by the Zhejiang Natural Science Foundation of China under Grant R18F010008, in part by the Natural Science Foundation of Ningbo under Grant 2017A610112, and in part by Ningbo University through the K. C. Wong Magna Fund.

ABSTRACT To enhance the depth perception for stereoscopic image retargeting, this paper presents a depth-adjustable stereoscopic image retargeting method via pixel fusion technique. The traditional methods enforce the depth-preserving constraint on the left and right images with poor depth adaption. To solve this issue, we try to address two critical properties that how to change the widths of unmatched region to control the depth perception, and how to change the alignment of left and right seams to satisfy visual comfort limits, and thus propose a seam manipulator tool to optimize the process for scaling factor determination of stereoscopic seams. The important contribution of our method is to take scaling preservation energy and disparity consistency energy into optimization. The experimental results demonstrate that our method can achieve promising performances on depth perception and visual comfort adjustment for better visual experience.

INDEX TERMS Stereoscopic image retargeting, pixel fusion, seam carving, visual comfort, depth perception, seam manipulation.

I. INTRODUCTION

With the rapid development of various stereoscopic 3D display devices, ranging from 3D televisions to mobile phones, requirements for 3D content manipulation with different aspect ratios and resolutions are becoming increasingly urgent [1]–[3]. Although the traditional cropping and scaling operators can fulfill the adjustment for stereoscopic images, how to maintain the binocular symmetries with proper 3D perception and comfortable viewing experiences is still challenging. In this paper, we focus on solving this issue via*depth-adjustable stereoscopic image retargeting*, that allows users to manipulate the scene's depth range to a comfortable perceived depth range, as well as the aspect ratios and resolutions.

The issue of 2D image retargeting has been widely researched over the past years. As broad classification of the existing approaches, discrete approaches [4]–[8], including seam carving and cropping, resize an image by iteratively removing or inserting pixels. However, discontinuous artifacts may be produced in the visually important regions due to the shortcomings of discrete approaches. In contrast, continuous approaches [9]–[13], such as mesh warping, aim to distribute more distortion on those less important regions and less distortion on those more important regions by controlling the mesh deformation without discontinuous artifacts.

When it comes to stereoscopic images, such seam removal and mesh deformation imposed on the left and right views independently may cause some degree of binocular asymmetries, which may lead to incorrect 3D perception and uncomfortable viewing experiences. Therefore, two types of constraints are used in most methods to overcome the challenges: 1) Depth preservation constraints. The constraints are considered in some seam carving and mesh warping methods [14]–[16] to preserve the depths of original 3D scenes; 2) Depth adaption constraints. The constraints are found in some mesh warping methods [17]–[19] to adapt aspect

The associate editor coordinating the review of this manuscript and approving it for publication was Xian Sun.

ratios and depth ranges on different devices. Since optimizing the depths of all pixels in a seam is more challenging than only optimizing the depths of four vertices in the warping-based methods, depth adaption has not been well considered in those seam carving based stereoscopic image retargeting method.

In this paper, focusing on seam carving framework for stereoscopic image retargeting, we address two critical properties: *how to change the widths of unmatched region to control the depth perception*, and*how to change the alignment of left and right seams to satisfy visual comfort limits*, which has not been considered in the existing seam carving based stereoscopic image retargeting methods. To emphasize the two properties in the framework, we propose a seam manipulator, a tool to optimize the process for scaling factor determination of stereoscopic seams, which simultaneously takes scaling preservation energy and disparity consistency energy into an optimization framework. Thus, besides shape preservation, depth perception and visual comfort adjustments can be solved with promising effects.

The main contributions are three-fold: 1) We analyze the properties for depth preservation and visual comfort preservation and further propose the depth perception and visual comfort adjustment solutions in terms of these properties, which are ignored in existing seam carving-based retargeting methods; 2) The importance of each seam is calculated by combining content significance energy, region mask information and seam significance energy, while the existing methods are lack of such consideration; 3) More critically, scaling preservation energy and disparity consistency energy are simultaneously used to optimize scaling factors for depth perception and visual comfort adjustments, so that better visual experience can be obtained compared with those depth-preserving stereoscopic image retargeting methods.

In the remainder of this paper, we first review the related work in Section II, detail our method in Section III, and finally present results in Section IV and conclusions in Section V.

II. RELATED WORKS

A. DISCRETE IMAGE/VIDEO RETARGETING

As discussed, seam carving approach tends to produce discontinuous artifacts in the visually important content. Moreover, although seam carving is intuitive and effective for image retargeting, it is not easy to extend it to stereoscopic case: if seams are carved for each view independently, binocular symmetry will be influenced. Therefore, some hard constraints (e.g., depth preservation) are applied to left and right views for maintaining the stereoscopic properties unchanged.

Utsugi *et al*. [20] preserved the geometric consistency of stereo pair, that maintain or change the consistency by using corresponding seams or occluded seams. Basha *et al*. [14] added geometric constraints to keep geometric consistency of the stereo pair. The method takes the visibility relations between pixels in the image pair into account to minimize the visual distortion in each seam as well as the depth. Lu *et al*. [21] minimized the shape distortion and preserved object boundaries by creating new occlusions, and preserved disparity consistency by corresponding seam pixel selection. Lei *et al*. [15] extended pixel fusion to depth-preserving stereo image retargeting, which keeps the widths of occluded and only change the widths of matched regions to minimize the depth distortion in stereo image pair. In other seam carving-based stereoscopic image retargeting methods [22]–[26], the similar constraints are used to preserve important objects, and maintain the consistency between the left and right images.

B. CONTINUOUS IMAGE/VIDEO RETARGETING

As another promising solution for retargeting, continuous approaches aim to optimize mesh warping using different deformation and depth constraints. To preserve the depth of 3D scenes, Lin *et al*. [27] imposed disparity preservation and shape preservation constraints to control the object-coherence warping to consistently preserve the disparities and shapes of visually salient objects. Li *et al*. [16] also utilized region-based depth-preserving constraint to control the warping function based on depth distortion model, and used shape preservation constraint to preserve the shapes of salient objects. Yoo *et al*. [28] retained the stereo consistency of the retargeted images by matching the vertices of the grid and preserving the correspondence between them. The common characteristics of these methods are that depth-preserving constraint is enforced to maintain the original disparity/depth ranges.

In contrast, some warping-based methods impose depth adaptation functions to optimize the depth of 3D scenes. Chang *et al*. [17] used a set of sparse correspondences to control the warping functions by imposing depth-editing constraints, that can keep their disparity values consistent with the original values, or interactively edit the depths for depth adaptation purpose. Yan *et al*. [18] utilized the relationship between disparity editing and content editing to guide the warping model. By the warping model, the disparity values of a sparse set of correspondences are adjusted to be identical with the target disparity range. Besides the sparse correspondences, Shao *et al*. [19] imposed shape preservation, visual comfort preservation and depth perception preservation constraints simultaneously to ensure strong 3D perception and comfortable viewing experiences. In the method, users allow to optionally specify the viewing distance and disparity range to propagate the constraints. Furthermore, depth-adaptive and object-selective factors are involved into the warping framework in [29] to provide more flexible editing function.

C. DEPTH ADAPTION

Besides the above stereoscopic image retargeting operations to adjust the resolutions for size adaption, depth itself is an important dimension to adapt the depth ranges of different displays. Many works have been proposed in stereoscopic disparity/depth editing, such as perspective manipulation [30], stereoscopic composition [31], and stereoscopic synthesis [32]. To adjust the disparity/depth effectively for

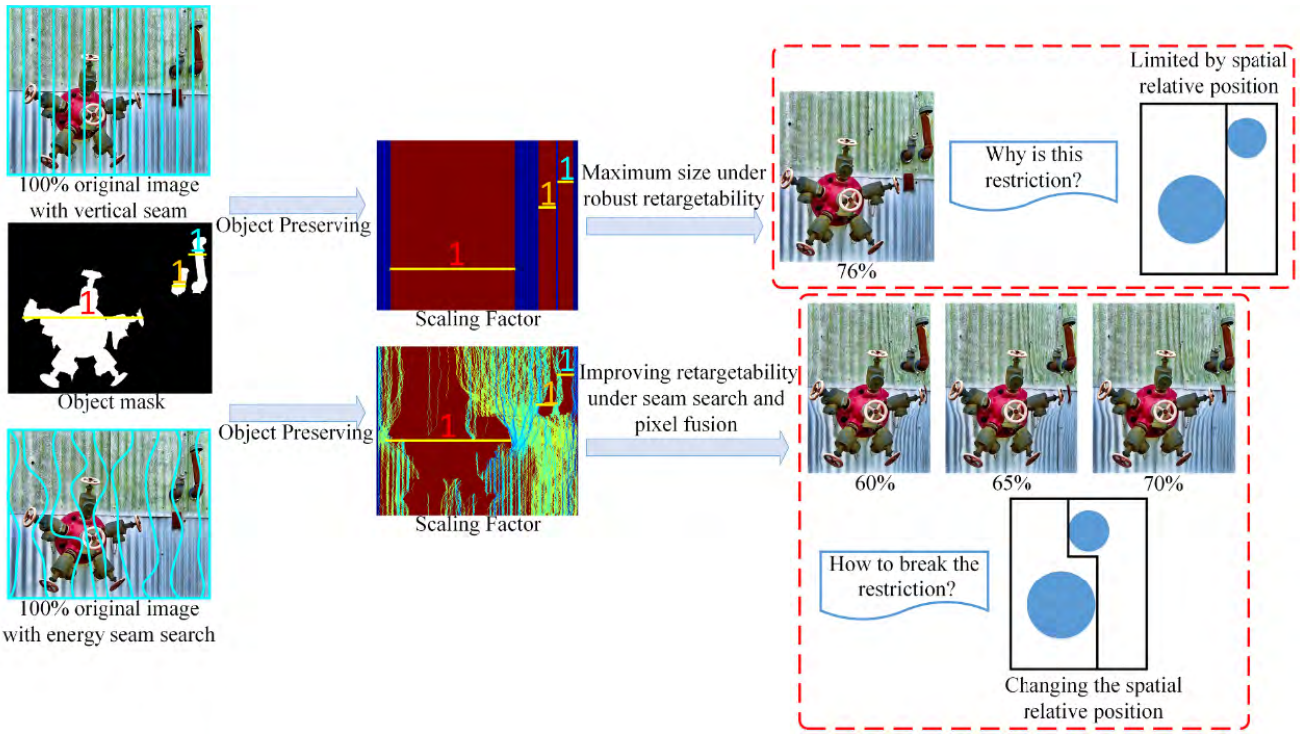

FIGURE 1. Motivation for seam manipulation.

stereoscopic 3D displays, warping methods are usually used for optimization. Lang *et al*. [33] proposed a series of disparity mapping operators for stereoscopic images and videos to change the disparity range. Yan *et al*. [34] proposed a linear depth mapping method through warping to change the depth range of a stereoscopic video on the basis of the viewing configuration. Wang *et al*. [35] proposed a mapping optimization method to adjust the disparity to minimize discomfort by warping-based manipulation. Yan *et al*. [18] proposed a content-aware stereoscopic mesh warping model to determine a scaling factor of salient region by disparity scaling factor. Lei *et al*. [36] proposed to adjust the 3D depth of an object by utilizing shape-preserving object depth control constraints. Besides using warping optimization, different disparity remapping functions were used to control the disparity range [37], [38].

D. MOTIVATION FOR SEAM MANIPULATION

Since each method has its advantage and disadvantage in retargeting stereoscopic images, it is unrealistic to propose a method that outperforms all other methods, thus the proposed method tries to absorb the advantages of other methods to enhance its performance. As discussed above, the advantage of seam carving is that the content of resizing is diverse due to the nature of graph cut (i.e., removing objects without artifacts), but the disadvantage is also obvious as it may lead to discontinuous deformation for removing pixels, while pixel fusion can solve the disadvantage by introducing inter-row importance filtering to ensure spatial coherence between adjacent rows. As shown in Fig. 1, compared with 0 and 1 scale of vertical seams, if we combine seam searching and pixel fusion, we can get a wider range of scale reduction while maintaining the scale of important objects. Mesh warping usually performs well in most cases, but it may produce inconsistent object deformation when the meshes deform seriously, while depth adaptation can be easily fused into the warping framework. Besides, since left-right consistency is established based on the vertices of the meshes, stereoscopic property preservation is not always better than seam carving based methods.

In this work, focused on the advantages of the existing image retargeting methods, we try to provide a new seam carving framework (united seam searching and pixel fusion) that can handle image retargeting, depth perception and visual comfort simultaneously. To optimize the scaling factor determination for depth adjustment purpose, we provide a seam manipulation solution to optimize the depth perception and visual comfort of the retargeted stereoscopic images for better visual experience, while the issue has not been studied in the existing seam caving based stereoscopic image retargeting methods [14]–[15], [20], [21]. Compared with those pixel fusion based methods [7], [15] and warping-based methods [17]–[19], the superiority of our method are validated on depth adaptation and a wider range of scaling.

III. PROPOSED METHOD

A. OVERVIEW

As discussed, pixel fusion is an effective solution to overcome the drawbacks of traditional pixel seam carving based image retargeting methods. Even though pixel fusion has

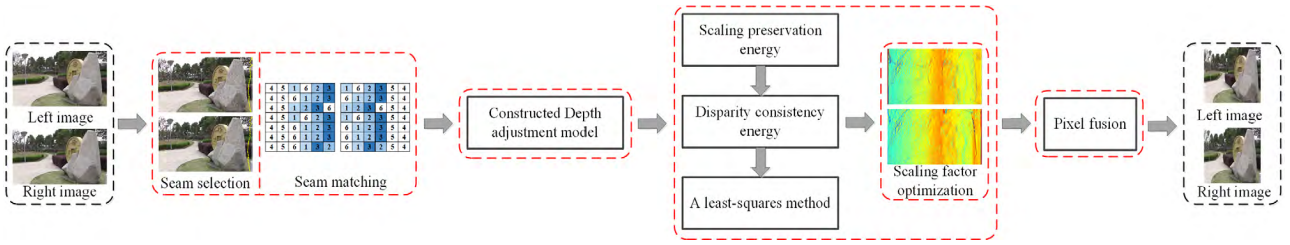

FIGURE 2. Procedure of our proposed scheme.

been adopted in 2D and stereoscopic image retargeting with promising performance [7], [15], the challenges for using pixel fusion in depth-adjustable stereoscopic image retargeting are that: 1) depth preserving constraint in [14]–[16] usually conflicts with depth adaptation in 3D display, especially ignoring visual comfort constraint, which motivates us to take visual comfort and depth sensation optimization simultaneously in pixel fusion for better visual experience; 2) scaling factor calculation in [7] and [15] aims to maintain higher scaling factors for those high-significance regions, especially scaling factor is set to 1 for unmatched regions, but the widths of unmatched regions can be changed to control the depth perception, which motivates us to change the definition of significance regions to control the scaling factors. Thus, aiming to solve these challenges, we propose a new depth-adjustable stereoscopic image retargeting method, named seam manipulator, to control the scaling factors for pixel fusion. Fig. 2 shows the procedure of our method, which mainly consists of four steps: seam selection and matching, depth adjustment model, scaling factor determination and pixel fusion. Next, we will demonstrate each step of the proposed method in details.

B. SEAM SELECTION AND MATCHING

As analyzed and revealed in our previous works [39], different regions in stereoscopic images demonstrate different binocular visual characteristics for perception, which should be imposed with different constraints for optimization in retargeting. In this work, we use stereo matching algorithm [40] to calculate the disparity map. Then, two classes of regions can be directly estimated from the disparity map:

Matched Region: A pixel in the left (right) view of a stereoscopic pair can find a corresponding pixel in the other view. The set of all matched pixels consists of matched region.

Unmatched Region: A pixel in one view cannot find any correspondence in the other view. The information is occluded or dis-occluded due to different viewing angles.

In seam carving based image retargeting method, the energy map plays a key role in determining the importance of each pixel for seam selection. A large significance value implies a low probability of a seam through the pixel, and vice versa. In this work, without specially designing significance energy construction, we directly use the algorithm in [14] to construct the energy map. Then, N_s seams are searched from the left image via dynamic programming optimization that minimizes the seam cost in a cost matrix formed from the energy map, where N_s is the number of all possible seams via seam searching. Note that, we set a large value for occluded pixels in the cost matrix to avoid the seam selection in the unmatched regions for the purpose of region preservation.

For stereoscopic image, seams in the left and right images should be coupled. However, directly using disparity map for seam matching will encounter visual distortion due to the influence of pixel's mismatching and un-matching. For example, multiple pixels in the left image may be mapped to the same pixel in the right image, and vice versa. In our seam coupling process, based on the order of seam selection, the first selected seam (all pixels in the seam) in the left image finds the matched seam in the right image using the disparity map. Then, the coupled seams are removed from the image pair, and the next coupled seams are searched and removed until all the seams are processed. By such operation, one-by-one seam coupling relationship can be established.

After the above seam coupling process, all pixels in each coupled seam will be assigned an ID ranging from 1 to N_s based on the order of seam selection. Except the pixels in the seams, the remaining pixels in each row will be also assigned an ID ranging from $N_s + 1$ to W, where W is the image width. For these pixels in the left image, the IDs are labeled sequentially from left to right, while the IDs are labeled from right to left in the right image, to reflect the inverse occlusion and disocclusion relationship between the left and right views. By such ID naming process, each pixel in the left image will have its matched pixel in the right image, even those occluded pixels are not actually matched via seam coupling. Then, the formed IDs are accomplished as matching map. The set of all vertical seams in a stereoscopic image pair is defined as below:

$$s = \{s_j^L, s_j^R\}_{j=1}^{W} = \{ID_j^L(i), ID_j^R(i)\}_{j=1}^{W} \tag{1}$$

where $ID_j^L(i)$ and $ID_j^R(i)$ are the corresponding IDs in row i and column j for the seams. In the description that follows, we use an ID to represent a seam. The important properties of the seam selection and matching scheme are that: 1) we do not make further change in the significant energy construction for seam searching, because our experiments find the influence can be compensated by the following scaling factors and pixel fusion; 2) we can obtain W seams equal to image width for

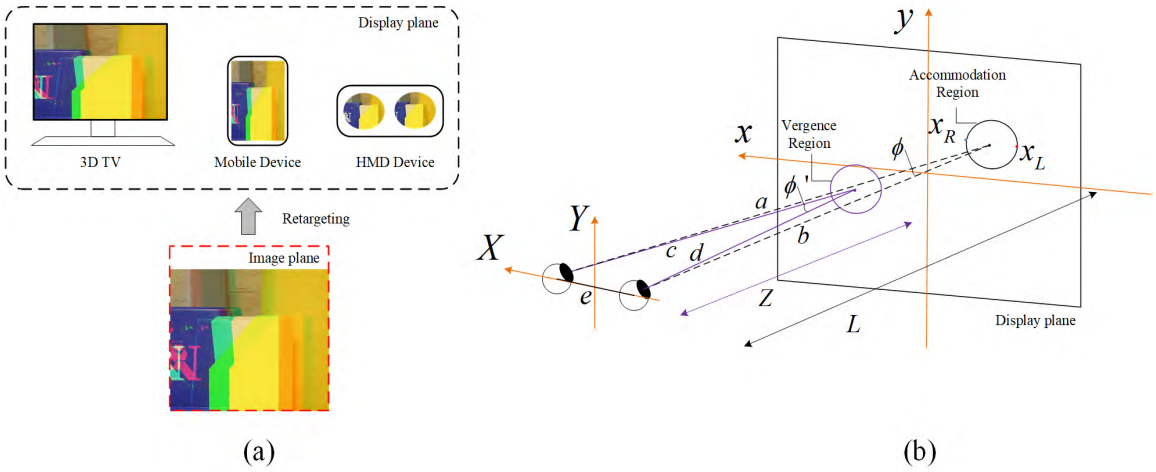

FIGURE 3. Illustration of camera geometry in (a) image plane (b) display plane.

each pixel based on the matching map, thus each seam has the importance for the subsequent scaling factor calculation, which is necessary in the pixel fusion based image retargeting using scaling factor as weights.

C. CONSTRUCTED DEPTH ADJUSTMENT MODEL

The purpose of image retargeting is to change the size of image content to adapt different display devices, while depth adaptation is an additional dimension to provide proper visual comfort and depth perception, which makes the case of stereoscopic image retargeting different with traditional image retargeting. For example, cinema screen has large display resolution, viewing distance and depth range, while 3D displays have relatively small display resolution and depth range. If directly displaying the cinema content on other 3D displays without depth adjustment, it will lead to poor depth perception and/or visual comfort. Therefore, depth adjustment is an important starting point in this work, which is different with the existing depth-preserving stereoscopic image retargeting methods [14]–[16]. In this work, we employ the zone of comfort to control depth adjustment. The typical zone of comfort is defined to be the range of $(-1°, 1°)$ [41]. The angular disparity is used here to control the depth. Fig. 3 (a) shows the stereoscopic geometry between image plane and display plane, and Fig.3 (b) shows the relationship between the estimated pixel disparity and angular disparity. It is more intuitive in the display plane to control the angular disparity range. For ease of understanding, we summarize some important notations and variables, as shown in Table 1. The second symbol in the first column denotes the target (adjusted) value.

Since display resolution is directly related to the resolution of displayed image content, a prior assumption is that the ratio between image resolution and display resolution before and after image resizing should remain unchanged with the form as follows:

$$\rho = \frac{R}{W} = \frac{R'}{W'} \tag{2}$$

TABLE 1. Important notations and variables.

Symbol	Definition
$W\,(W')$	Image resolution
$R(R')$	Display resolution
$d_D\,(\tilde{d}_D)$	Disparity on the image plane
$D_{DP}\,(\tilde{D}_{DP})$	Disparity on the display plane
$D_{AD}\,(\tilde{D}_{AD})$	Angular disparity in degree
$Z\,(\tilde{Z})$	Depth on the display plane
e	Distance between two eyes
L	Viewing distance in meters

Then, disparity in pixels (d_D) can be converted to disparity on the display (D_{DP}) by

$$D_{DP} = \rho \cdot d_D \tag{3}$$

By using this relationship, we can project the matched pixels (x_L, y) and (x_R, y) in a stereoscopic image ($x = (x_L + x_R)/2$, $d_D = x_R - x_L$) to the 3D space, obtaining their 3D coordinate (X, Y, Z) in the 3D space as follows:

$$X = \frac{e}{e - D_{DP}} \cdot x \tag{4}$$

$$Y = \frac{e}{e - D_{DP}} \cdot y \tag{5}$$

$$Z = \frac{e}{e - D_{DP}} \cdot L \tag{6}$$

Based on the location in (X, Y, Z), the angular disparity is obtained via

$$D_{AD} = \phi - \phi' = \arccos\left(\frac{a^2 + b^2 - e^2}{2ab}\right) - \arccos\left(\frac{c^2 + d^2 - e^2}{2cd}\right) \tag{7}$$

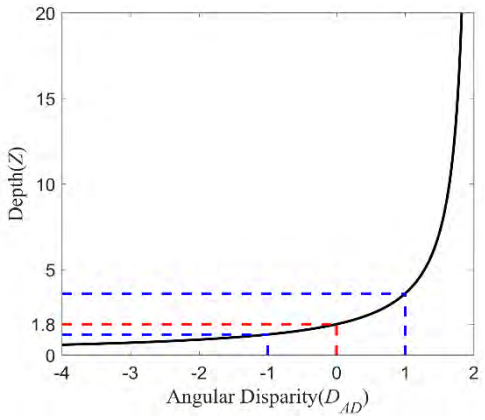

FIGURE 4. Relationship between D_{AD} and Z.

where $a = (L^2 + (X - e/2)^2 + Y^2)^{1/2}$, $b = (L^2 + (X + e/2)^2 + Y^2)^{1/2}$. If the object has negative disparity (popping-out the screen with $D_{DP} < 0$), then $c = (Z^2 + (X - e/2)^2 + Y^2)^{1/2}$, $d = (Z^2 + (X + e/2)^2 + Y^2)^{1/2}$. Otherwise (behind the screen with $D_{DP} > 0$), $c = (Z^2 + (X - e/2)^2 + Y^2)^{1/2}$, $d = (Z^2 + (X + e/2)^2 + Y^2)^{1/2}$.

In order to ensure visual comfort, the regions exceeding the zone of comfort limits should be adjusted. Different with our previous works directly operating on the perceived depth to match such limits [42], in this work, we use a more intuitive scheme that directly maps angular disparities into the $(-1°, 1°)$ limits. As shown in Fig. 4, by observing the relationship between D_{AD} and Z, Z increases very fast when $D_{AD} > 0$, while the increase is relatively slow for $D_{AD} < 0$. Therefore, to reduce the sensitivity of depth change, we do not change the depth layout of the whole scene (e.g., object popping-out the screen is still in the front display plane). Generally, we can map the angular disparity into a new target one by

$$\tilde{D}_{AD} = \begin{cases} \dfrac{D_{AD} - D_F}{D_F - D_N}, & \text{if } D_F < 0 \\ \dfrac{D_{AD} - D_N}{D_F - D_N}, & \text{if } D_N > 0 \\ \dfrac{2D_{AD} - (D_N + D_F)}{D_F - D_N}, & \text{otherwise} \end{cases} \tag{8}$$

where D_F and D_N are the farthest and nearest angular disparities in the original stereoscopic image. Particularly, for those pixels in the unmatched regions, the angular disparities are all set to zero, indicating monocular visual perception for these regions.

After obtaining the adjusted angular disparity ($\tilde{D}_{AD}$), we can inversely solve a quartic equation from Eq. (7) to obtain the adjusted depth ($\tilde{Z}$), and then obtain the adjusted disparity on the display plane ($\tilde{D}_{DP}$) by Eqs. (3) and (6). Based on the same assumption in Eq. (2) that the original and resized images have the same ratio between image resolution and display resolution, we can easily obtain the adjusted pixel disparity. Thus, by the above steps, the target disparity map for an input stereoscopic pair can be obtained to indicate the disparity constraint for left-right consistency. In this paper, we use the assumption in Eq. (2) to optimize the image resolution for better display adaptation.

D. SCALING FACTOR DETERMINATION

With the above matching map calculation, each pixel in the left or right image will assign a scaling factor to indicate the degree of resizing in the next pixel fusion based retargeting operation. However, for stereoscopic vision, depth perception from monocular occlusion (unmatched regions) and binocular disparity (matched regions) is occurred simultaneously. The phenomenon of depth perception from monocular occlusion is known as da Vinci stereopsis [43]. In the previous stereoscopic image retargeting works [25], to preserve depth perception, the widths of unmatched regions remain unchanged, while only the widths of matched regions are changed. However, for depth adjustable stereoscopic image retargeting, the widths of unmatched regions should be adjusted correspondingly to adapt the new imaging geometry. Therefore, as the first depth-adjustable property in our method, we have the following observation:

Property 1: The essence of depth preservation is to maintain the widths of unmatched regions, i.e., we can reduce the widths of unmatched regions to alleviate depth perception, or inversely increase the widths of unmatched regions to boost depth perception.

To address such property in depth preservation, we introduce a region mask to represent the matched/unmatched regions and the degree of depth preservation in determining the scaling factor for those regions, which is defined as follows:

$$Mask = \begin{cases} 0, & \text{unmatched regions} \\ 1, & \text{otherwise} \end{cases} \tag{9}$$

From another perspective, the importance of each seam is directly related to the content significance of the pixels. The 3D saliency detection model [44] is used to generate the content significance energy. Secondly, in the matching map calculation, each coupled seam has been assigned an ID. The ID also represents the order of the seam in calculating the matching map. Since the principle of seam selection is to avoid crossing the important regions, the seams with small IDs normally have small importance in representing image content. Therefore, we design another seam significance energy to indicate such property, in which pixels that do not belong to the matched regions are assigned a small or large constant to indicate the cases of depth adjustment, i.e.,

$$E_{ID}(x, y) = \begin{cases} \sqrt{ID(x, y)/N_s}, & \text{if } (x, y) \text{ is matched} \\ 0, & \text{otherwise} \end{cases} \tag{10}$$

Then, the importance map is calculated by combining the content significance energy, region mask information and seam significance energy as follows:

$$M = \beta \cdot S_{3D} + \gamma \cdot Mask + \eta \cdot E_{ID} \tag{11}$$

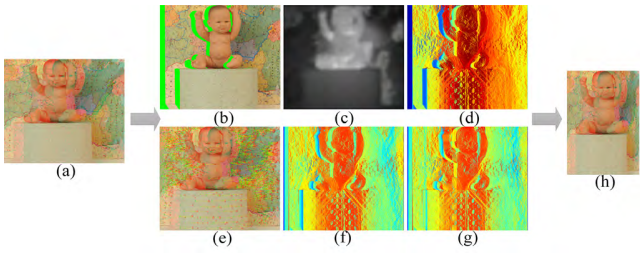

FIGURE 5. Examples of scaling factor maps. (a) Input image. (b) Region mask map (green region). (c) Content significance map. (d) Seam significance map. (e) Feature point matching map. (f) Scaling factor map after optimization. (g) Scaling factor map after post-processing. (h) Output image.

where parameters β, γ and η denote the weights for the energy terms, satisfying $\beta + \gamma + \eta = 1$. In the experiment, we set $\beta = 0.55$, $\gamma = 0.30$ and $\eta = 0.15$. Figs. 5(b)-(d) show the mask map (green region), content significance map (3D saliency) and seam significance map for the input image in Fig. 5(a).

Finally, the importance of each seam is given as:

$$IM_j = \frac{\sum_{i=1}^{H} M_j(i)}{H} \tag{12}$$

where IM_j denotes the importance of the j-th seam, $M_j(i)$ denotes the importance value on the i-th row in the j-th seam, and H is the height of image. Compared with seam's importance construction in previous works [7], [15], our importance map adds additional seam region mask and significance energy to change the distributions in force.

However, only changing the widths of matched/unmatched regions cannot reach satisfactory visual experience for user due to the lack of visual comfort constraint. That is, by changing the widths of matched/unmatched regions, the degree of visual comfort cannot be measured and restricted, thus another constraint is needed to change the depth of matched regions to avoid accommodation and convergence conflict (to satisfy zone of comfort limits). Therefore, as the second depth-adjustable property in our method, we have the following observation:

Property 2: The essence of visual comfort preservation is to maintain binocular alignment with the zone of comfort limits, i.e., we can change the alignment of left and right seams to satisfy the limits.

As discussed above, even we can reduce the width of unmatched regions to adjust the depth perception, the visual comfort of the adjusted image is still uncontrollable. Therefore, as an important semantic for user's visual experience, this property is complementary with the first property to characterize visual comfort and depth perception in 3D Quality of Experience (QoE).

Based on the above discussed properties for stereoscopic image retargeting, the goal of scaling factor calculation motivated in this work is to change the degree of resizing for each pixel, which should: 1) maintain higher scaling factors for those high-significance objects; 2) change the distributions of the matched seams in the left and right views to adapt the adjusted depth. Based on these considerations, we define the following energy terms to supervise scaling factor calculation.

Similar with warping-based image retargeting [17]–[19], to preserve the high-significance objects as much as possible, while allow to large deformation for those low-significance objects, scaling factors for different seams are adjusted to satisfy the requirement. In this work, to address the inconsistent deformation via scaling factor, the distance between the measured scaling factor and its benchmark value is calculated. Here, the benchmark scaling factor is set to 1 to maintain the width of the object. Thus, we have the scaling preservation energy term as:

$$E_{SP} = \sum_{j=1}^{W} IM_j^L \cdot |Scal_j^L - 1| + \sum_{j=1}^{W} IM_j^R \cdot |Scal_j^R - 1| \tag{13}$$

where IM_j^L and IM_j^R are the significance values of the j-th seams in the left and right images, respectively, $Scal_j^L$ and $Scal_j^R$ are the scaling factors of the j-th seams in the left and right images, respectively.

However, the above energy term only considers the region importance for scaling preservation. To ensure the adjusted scaling factors of all matched seems to be consistent with the expected target disparities, their distributions (reflected by the sum of scaling factors) should be adjusted to match the target disparities. However, it is unrealistic to adjust the accumulative scaling factors for each pixel due to high complexity, thus we extract Speeded-Up Robust Features (SURF) features from the left and right images, and use Random Sample Consensus (RANSAC) to ensure binocular alignment consistency between the left and right images, as shown in Fig. 5(e). Let (τ_k^L, τ_k^R) be a pair of matched points in the left and right images, $(\tau_k^L, \tau_k^R) \in \Omega$, the disparity consistency energy term is defined as:

$$E_{DC} = \sum_{(\tau_k^L, \tau_k^R) \in \Omega} \left((\sum_{j=1}^{\tau_k^L} Scal_j^L - \sum_{j=1}^{\tau_k^R} Scal_j^R) - \tilde{d}_{\tau_k^L} \right) \tag{14}$$

where $\tilde{d}_{\tau_k^L}$ is the target pixel disparity for the feature point τ_k^L in the left image estimated in the above depth adjustment step. Thus, with this energy term, the scaling factors in the left and right images are simultaneously adjusted to satisfy the disparity consistency constraint.

With the scaling preservation energy term E_{SP} and disparity consistency energy term E_{DC}, depth perception and visual comfort are simultaneously adjusted to characterize the above two properties. The objective function can be formulated as:

$$\begin{aligned} &\arg\min (E_{SP} + \lambda \cdot E_{DC}) \\ &\text{s.t.} \begin{cases} \sum_{j=1}^{W} Scal_j^L = W', \quad 0 \le Scal_j^L \le \delta \\ \sum_{j=1}^{W} Scal_j^R = W', \quad 0 \le Scal_j^R \le \delta \end{cases} \end{aligned} \tag{15}$$

where W and W' are widths for the original and resized images, respectively, having $W'/W < 1$ to reduce the image width, δ is a parameter to control the strength of scaling factor, and λ is the weight for the latter term. In the experiment, we set $\lambda = 0.25$, and a small value ($\delta = 1$) for the case of disparity decreasing and a large value ($\delta = 2$) for the case of disparity increasing. The above equation can be solved by a least-squares method.

After the above optimization, a set of scaling factors for the left and right images are obtained. The blue regions in Fig. 5(d) are more necessary to be adjusted than the red regions. As shown in Fig. 5(f), the scaling factors after optimization are generated, and the importance of different regions can be reflected by the scaling factors. However, since only the scaling factor for each vertical seam is considered in this work, shape deformation will be appeared in the horizontal direction (it is also obvious in the vertically adjacent scaling factors in Fig. 5(f)). To eliminate such influence, we add a post-processing operation to filter the scaling factors. Let $Scal(i,k)$ denotes the scaling factor for a pixel (i,k), by finding an optimal column j that satisfies $std\{Scal(i,k)|1 \le i \le H, 1 \le k \le j\} > \eta$ for all the pixels below the column, where $std\{\}$ denotes standard deviation operation, we calculate a compensation factor for each row starting from $g = 1$ as follows:

$$e_i = \sum_{k=g}^{j} Scal(i,k) - \sum_{i=1}^{H}\sum_{k=g}^{j} Scal(i,k)/H \tag{16}$$

Then, for all pixels in the i-th row, the adjusted scaling factor is calculated as:

$$Scal(i,k) = \begin{cases} Scal(i,k) - e_i/(j-g+1), & \text{if g} \le k \le j \\ Scal(i,k) + e_i/(W-j), & \text{if } j+1 \le k \le W \end{cases} \tag{17}$$

The above process is iterative by updating $g = j + 1$. To facilitate understanding, we summarize the process of seam alignment in Algorithm 1. As shown in Fig. 5 (g), after post-processing operation, scaling factors within a certain range will be comparatively smooth, leading to continuous shape of the important object (it is obvious in the following results as compared with seam carving methods).

E. PIXEL FUSION

After obtaining the scaling factor for each pixel in the left and right images, the resized images can be generated using the pixel fusion algorithm [45]. The essence of pixel fusion is to interpolate the resized pixels using scaling factor as weights. In this work, we directly apply the pixel fusion algorithm on the left and right images respectively. An important point deserved to address here is that, since the generated scaling factors have contained the geometry of binocular vision, no further optimization is necessary for the retargeted stereoscopic pair.

Algorithm 1 Seam Alignment

Input: Optimized scaling factor: *Scal*;
Initial position: $g = 1, j = 1$;
The width and height of image: W and H;
Pixel inconsistency of maximum tolerable in the row: η
Output: New scaling factor: *Scal*;
1: for $j = 1$ to W
2: **if** $e_i > \eta$ and $g < W$ in Eq. (16)
3: Update *Scal* ← Compute the new *Scal* using Eq. (17);
4: **end**
5: $g = j+1$ ← Compute the new starting column for the next cycle;
6: end
7: Return *Scal*;

IV. EXPERIMENTAL RESULTS

In this section, to demonstrate the performance of the proposed method compared with the existing methods, we collect the testing stereoscopic images from the following datasets: NBU 3D-VCA image dataset [46], IVY LAB Stereoscopic 3D image database [47] and Middlebury stereo dataset [48]. In the experiment, we set the interocular distance $d_e = 65$mm, the viewing distance $L_D = 1800$mm, and the disparity limits $(-1°, 1°)$. We make the results publicly available at https://pan.baidu.com/s/1xpQ3GfjvGzBWlKvYCQwOtQ. Note that, for different disparity limits or viewing distances, the retargeting performance will be influenced.

A. COMPARISON WITH SEAM CARVING BASED METHODS

We compare our method with three state-of-the-art seam carving based stereoscopic image retargeting methods, including geometrically consistent stereoscopic seam carving approach (GASSC) [14], pixel fusion based stereoscopic image retargeting approach (DPSPF) [15], and visual attention guided stereoscopic seam carving approach (VASSC) [25]. These approaches are all seam carving based approaches that still preserve the original depth range after retargeting. A qualitative comparison of the retargeting results on three stereoscopic images with relatively small depth range are presented in the left side of Fig. 6. All images are shrunk by 40%. From the figure, the seam carving methods will suffer from serious object shape deformation, e.g., the flower in (e), the street lamp in (c) and the wheels in (c). In contrast, since the disparity consistency energy and scaling preservation energy are simultaneously considered, our method not only preserves the shape of the important object, but also enhances the depth sensation for these stereoscopic image pairs with small depth range (the depth range is adaptively expanded). The phenomenon is very obvious in the corresponding disparity maps. Note that, since we do not particularly design the significance energy construction for seam selection and 3D saliency calculation in importance map construction, our method may be not prominent in object

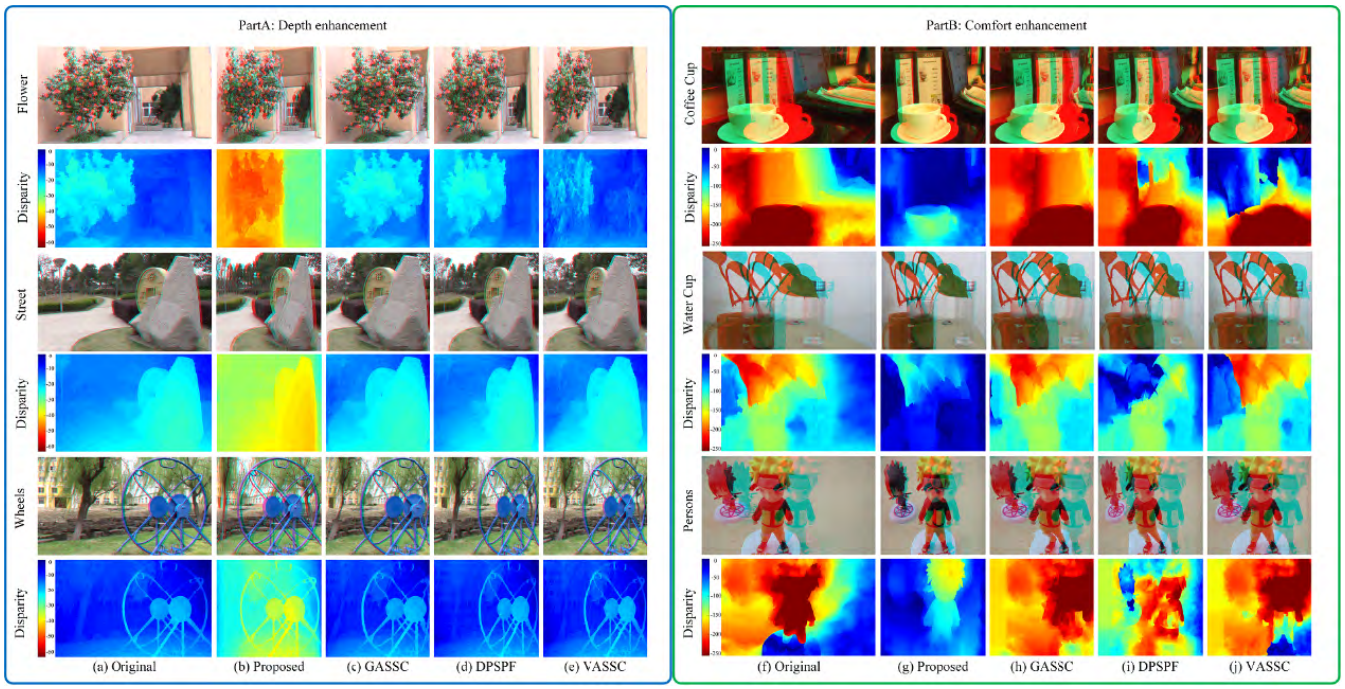

FIGURE 6. Results on six stereoscopic image pairs (left side: three image pairs of small depth range; right side: three image pairs of large depth range). From top to bottom in each subgraph: the retargeted stereoscopic images (shown in red-cyan anaglyph) and the disparity maps (shown in pseudo-color map).

preservation compared with other methods, but the target for adaptive depth perception and visual comfort adjustments can be achieved.

In addition, we also illustrate the retargeting results on three stereoscopic image pairs with large depth range in the right side of Fig. 6 (the stereoscopic images are visually uncomfortable). Similar with the conclusion above, GASSC and DPSPF methods will deform the shapes of the coffee cups in (h) and (i), the water cups in (h) and (i), and the person's legs in (h) and (i). More importantly, their large depth ranges are outside the zone of comfort, which leads to poor visual comfort experience. All these methods enforce disparity/depth preservation constraint. In conclusion, the seam carving methods may lead to shape deformation due to irregular seam removals, especially under large shrinking ratio (also very clear in the following comparison results), while the proposed method takes scaling preservation energy and disparity consistency energy into account, achieving better user's visual experience. The results on Middlebury stereoscopic image pair in Fig. 7 also have the similar conclusion in shape preservation, depth perception and visual comfort adjustments.

B. THE NECESSITY AND EFFECTIVENESS OF SEAM ALIGNMENT

In order to investigate the influence of seam alignment on disparity range and image quality, we show the retargeting results with different thresholds η in Fig. 7(b). Taking $\eta = \infty$ as ground truth (i.e., without seam alignment), for increasing η, the disparity value is becoming closer to the ground truth,

TABLE 2. Loss of angular disparity and scaling factor.

Metric	η=5	η=6	η=7	η=8	η=9	η=10
D_{AD}-Loss	0.125	0.117	0.135	0.081	0.082	0.104
Scal-Loss	0.047	0.042	0.038	0.037	0.035	0.032

but the image quality is also degraded. We calculate the correlation coefficient (CC) for angular disparities and scaling factors between ground truth and different thresholds η. As shown in Fig. 8. although the CC of angular disparity (0.95 on average) is slightly lower than the scaling factor (0.98 on average), this may be related to the accuracy of disparity estimation. A high CC indicates that seam alignment improves image quality without large deviations from previous optimization results (salient object preservation and disparity adaptation). Meanwhile, we calculate the specific loss at the pixel level in Table 2, where the average loss of angular disparity is 0.107 and the average loss of scaling factor is 0.039. For balancing the two effects of disparity range and image quality, $\eta = 6$ is set in our experiment, where CC is beyond 0.95 both in aspects of angular disparity and scaling factor.

C. RESULTS WITH DIFFERENT SHRINKING RATIOS FOR IMAGE RESIZING

The drawback of the existing seam carving based retargeting methods is that seam removal will produce discontinuous artifacts in the visually important content, especially with large image shrinking, while pixel fusion can effectively

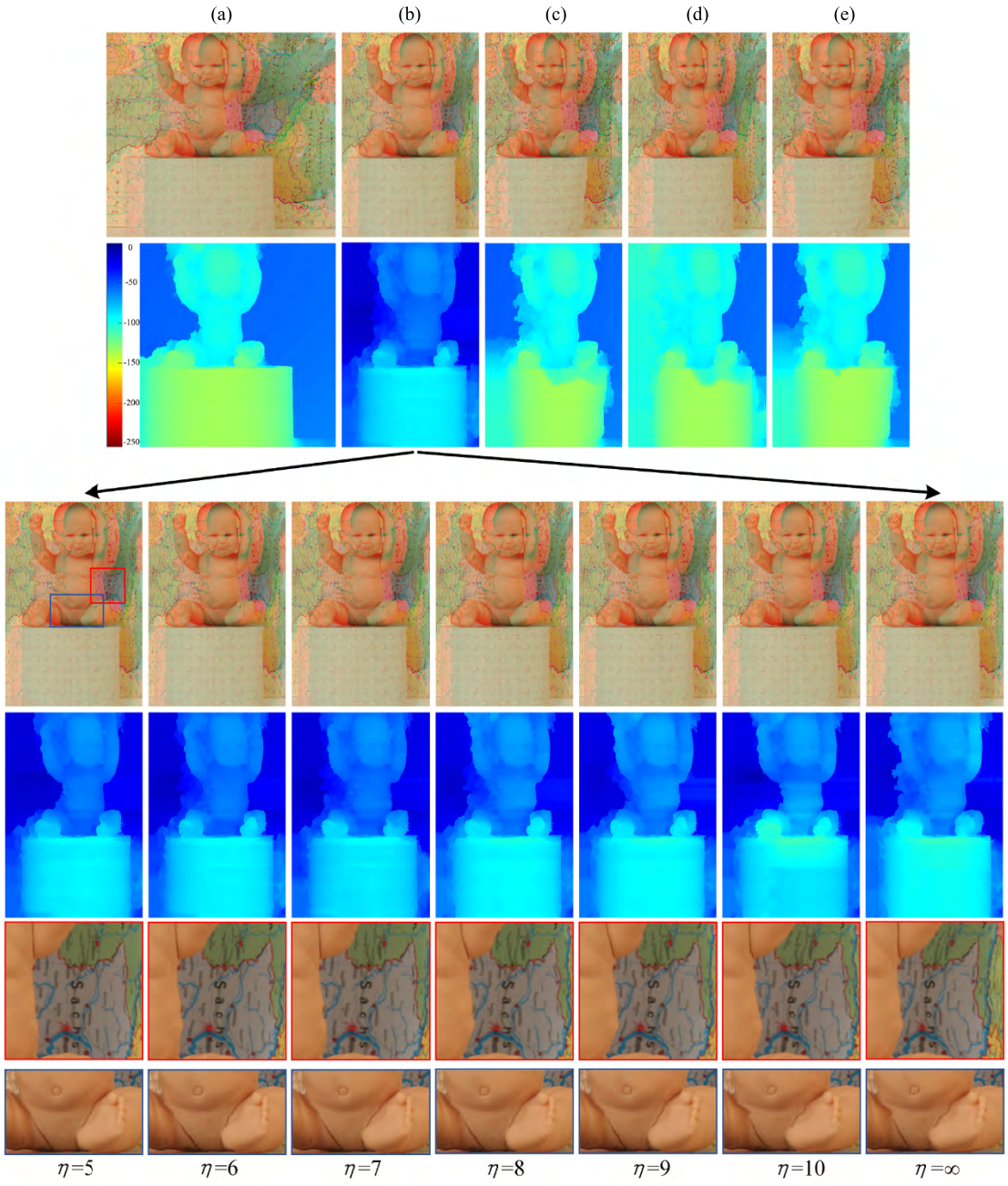

FIGURE 7. Results on one middlebury stereoscopic image pair. From top to bottom in each subgraph: the retargeted stereoscopic images (shown in red-cyan anaglyph), the disparity maps (shown in pseudo-color map), and the detail of (b) about the influence of seam alignment.

eliminate such discontinuity by introducing inter-row importance filtering. To address such point, we show the retargeting results of our seam manipulator for shrinking image width by 60%, 40%, 20%, and -20% in Fig. 9, in comparison with other seam carving based methods (GASSC, DPSPF and VASSC). Here, shrinking image width by -20% denotes to add the image width to 120% of its original width. From the results, we find these comparison methods have serious shape deformation in lower shrinking ratio (e.g., 40%), while our method still has promising retargeting results under the lower ratio. With the decreasing ratio for shrinking, these comparison methods will have good shape preservation performance, but depth adaptation for these methods is still poor due to the depth preservation essence.

D. THE INFLUENCE OF DEPTH PERCEPTION AND VISUAL COMFORT CONSTRAINTS

Since our method uses the scaling preservation energy and disparity consistency energy terms to manipulate the seams, the impact of each energy term should be proved.

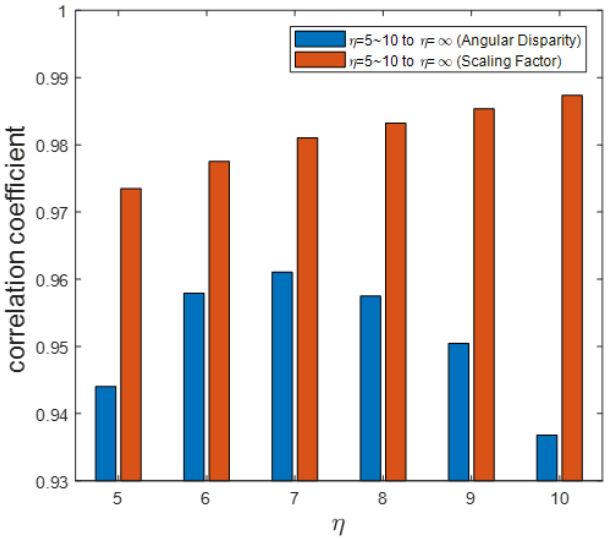

FIGURE 8. The effect of seam alignment.

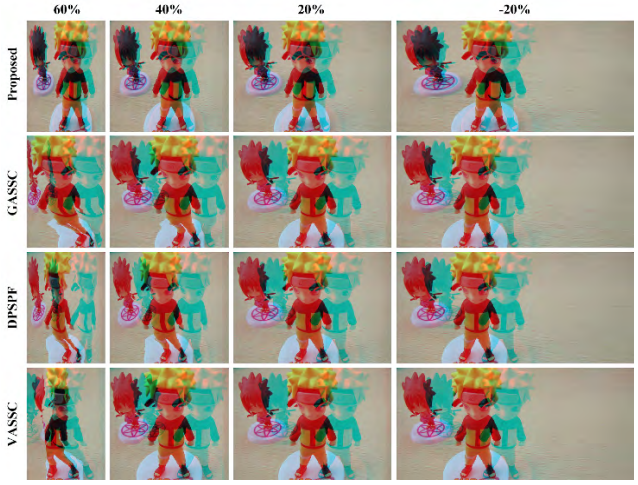

FIGURE 9. Comparisons of the retargeting results for shrinking the image width by: 60%, 40%, 20%, and −20%.

We design the following schemes for comparison listed in Table 3, denoted by Scheme-1, Scheme-2, Scheme-3 and Proposed scheme, respectively. The retargeting results are shown in Fig. 10. Three important conclusions can be drawn from the results: 1) only with the scaling factors calculated in Ref. [15], the width of the unmatched regions is preserved to maintain the original depth perception in "Street" of Fig. 6; 2) compared with Scheme-2 and Proposed scheme with or without E_{DC}, the added disparity consistency energy term will largely affect the overall depth range. That is, only using scaling preservation energy term will seriously deteriorate the depth perception with extremely low depth range; 3) compared with Scheme-3 and Proposed scheme with or without E_{SP}, although their depth ranges are similar, the size of the important object (e.g., the foreground sculpture) is adaptively scaled with the scaling preservation energy term. Therefore, we can conclude that

TABLE 3. List of the schemes compared in this study.

Method	Description
Scheme-1	Only with initial scaling factors in Ref. [15]
Scheme-2	Only with E_{SP} in Eq. (13)
Scheme-3	Only with E_{DC} in Eq. (14)
Proposed	With both E_{SP} and E_{DC} in Eq. (15)

TABLE 4. The user's preference results of subjective paired comparisons.

Method \ Images	Part A in Fig.6			Part B in Fig.6			Avg
	#1	#2	#3	#4	#5	#6	
GASSC	72%	84%	96%	92%	96%	84%	87.3%
DPSPF	68%	76%	88%	92%	96%	84%	84.0%
VASSC	88%	84%	96%	84%	92%	76%	86.7%

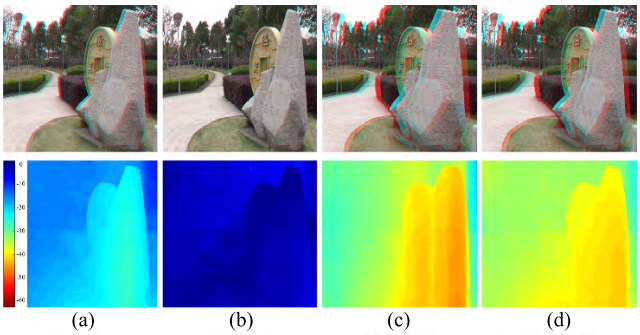

FIGURE 10. Comparisons of the retargeting results with different schemes.

cooperation of disparity consistency energy and scaling preservation energy terms will provide more natural subjective perception for users than only considering a single energy term.

E. QUANTITATIVE RESULTS

1) USER STUDY

Refer to our previous subjective testing [19], we also perform a similar user study to assess our algorithms. The subject test was also conducted in the Lab designed for subjective quality test at Ningbo university. The test environment and condition met ITU-R BT.500-11 [49]. 25 participants were participated in our user studies. We conduct subjective experiment on a Samsung UA65F9000 65 inch Ultra HD 3D-LED TV with 3D shutter glasses, in which paired comparisons between the retargeted results obtained by our method and one of the comparative methods (GASSC [14], DPSPF [15], or VASSC [25]) are conducted according to Double Stimulus Continuous Quality Scale (DSCQS) test methodology. In the test, 6 stereoscopic image pairs in Fig. 6 (#1∼6 represents 6 scenes from top to bottom) are chosen for test. Each participant is asked to give his own preference about if the retargeted result obtained by our method is better than the other result according to the overall visual experience in terms of shape preservation, depth perception and visual comfort. The user study results are reported in Table 4. It is clear that our

TABLE 5. Objective evaluation results for different methods.

Metric	Different methods			
	GASSC	DPSPF	VASSC	Proposed
PGDIL	0.298	0.444	0.338	**0.710**
ARS	0.773	0.789	0.760	**0.805**

method gets higher preference votes for these test images than the other three methods. On the contrary, even better shape preservation can be achieved for the comparison methods in some testing images, depth adaption is still poor on the cases with large and small depth ranges, leading to poor viewing experience.

2) OBJECTIVE EVALUATION

We use PGDIL [50] and ARS [51] as objective metrics to evaluate the retargeted results obtained by our method. PGDIL evaluates the visual quality of retargeted images by measuring the geometric distortion via the local variance of SIFT flow and measuring the information loss via the saliency map, while ARS evaluates the retargeted images by exploiting the local block changes. As shown in Table 5, focused on geometric distortion and information loss in these metrics, our method is superior to other comparison methods.

F. COMPARISON WITH WARPING-BASED METHODS

As discussed, the motivation of the proposed method is to absorb the advantage of those continuous approaches (to make the seams continuous). For objective evaluation, we also report the comparison results with two warping-based methods: content-aware display adaptation approach (SLWARP) [17], and QoE-guided warping approach (QoEWARP) [19]. All images are resized to 40% of original width. As shown in Fig. 11, although under such large scaling ratio, our method still has acceptable performance in comparison with the two methods. Especially SLWARP method will lose the boundary contents and produce inconsistent object deformation when the meshes deform seriously. For QoEWARP method, to preserve the size of object, deformation on an object will be inconsistent, leading to lower completeness. Overall, compared with the discrete (seam carving based) methods, our method can achieve smaller resizing while still having better visual quality, while compared with continuous (warping based) methods, our method can obtain better performance in object completeness. Therefore, to involve the advantages of discrete and continuous methods, how to make a better tradeoff between discrete and continuous properties is still worthy of further study.

G. COMPUTATIONAL COMPLEXITY

To further analyze the computational complexity of the proposed method, we compare the run-time costs in

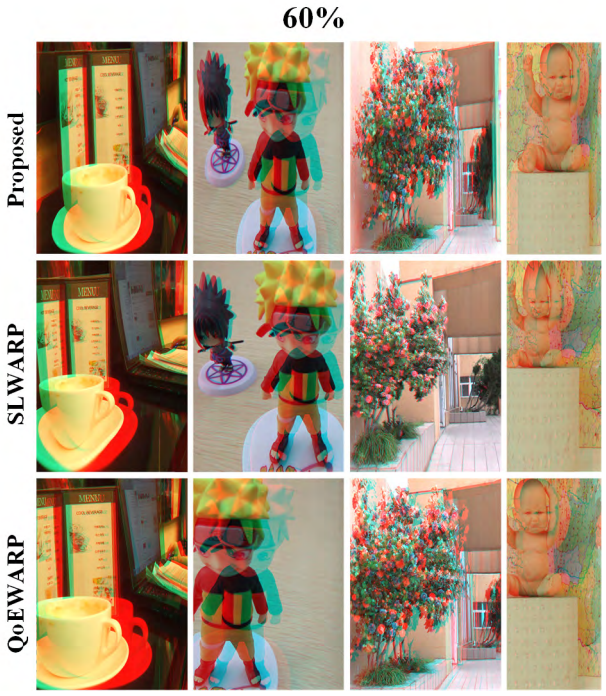

FIGURE 11. Comparisons of the retargeting results with warping-based methods. From top to bottom: the retargeted stereoscopic images with the proposed method, SLWARP method, and QoEWARP method.

TABLE 6. Average computational cost for a stereoscopic image.

Metric	Different methods			
	GASSC	DPSPF	QoEWARP	Proposed
Time (s)	80.13	92.04+10.46	3.31	92.04+23.26

resizing 40% of original width (the average runtime for a stereoscopic image with resolution of 500 × 375) in Table 6. The test platform is Intel Core(TM) i5-4200M CPU @ 2.50 GHz with MATLAB compiler. Observed from the result, QoEWARP method will have low computational cost compared with other three methods, because it does not need the complex seam searching process. The complexity of GASSC method is high because it should search the maximum seams related to the scaling ratio. The complexity of DPSPF method and our methods is high (the processing of seam selecting and the processing after the seam selecting), because pixel fusion guided methods must search and select all possible seams from whole image no matter how small or large scaling ratio is used. According to statistics, pixel fusion will occupy about 80% of the overall time complexity in our method. Therefore, focusing on using the traditional seam carving framework to promote user's visual experience for stereoscopic image retargeting, computational efficiency of our method is not high, but it has large space for promotion via effective parallel computation for seam searching and fusion to make the technique more practical.

V. CONCLUSIONS

In this paper, we present a new depth-adjustment stereoscopic image retargeting method, which leverages pixel fusion to investigate how to change the widths of unmatched region to control the depth perception, and how to change the alignment of left and right seams to satisfy visual comfort limits. Thus, new scaling preservation energy and disparity consistency energy are designed to optimize the process of scaling factor determination. As a result, our method yields a retargeted result with better visual experience to adjust the depth perception and visual comfort. In future work, we plan to consider additional depth-adjustable properties (e.g., vergence and accommodation) simultaneously. We also plan to extend this framework to enable new role in discrete and continuous approaches [52].

REFERENCES

[1] O. Wang, M. Lang, M. Frei, A. Hornung, A. Smolic, and M. Gross, "StereoBrush: Interactive 2D to 3D conversion using discontinuous warps," in *Proc. 8th Eurograph. Symp. Sketch-Based Inter. Modeling*, 2011, pp. 47–54.

[2] Y. Niu, F. Liu, W.-C. Feng, and H. Jin, "Aesthetics-based stereoscopic photo cropping for heterogeneous displays," *IEEE Trans. Multimedia*, vol. 14, no. 3, pp. 783–796, Jun. 2012.

[3] W. Wang, J. Shen, Y. Yu, and K.-L. Ma, "Stereoscopic thumbnail creation via efficient stereo saliency detection," *IEEE Trans. Vis. Comput. Graphics*, vol. 23, no. 8, pp. 2014–2027, Aug. 2017.

[4] S. Avidan and A. Shamir, "Seam carving for content-aware image resizing," *ACM Trans. Graph.*, vol. 26, no. 3, 2007, Art. no. 118.

[5] M. Rubinstein, A. Shamir, and S. Avidan, "Improved seam carving for video retargeting," *ACM Trans. Graph.*, vol. 27, no. 16, 2008, Art. no. 16.

[6] M. Grundmann, V. Kwatra, M. Han, and I. Essa, "Discontinuous seam-carving for video retargeting," in *Proc. Int. Conf. Comput. Vis. Pattern Recognit. (CVPR)*, Jun. 2010, pp. 569–576.

[7] B. Yan, K. Li, X. Yang, and T. Hu, "Seam searching-based pixel fusion for image retargeting," *IEEE Trans. Circuits Syst. Video Technol.*, vol. 25, no. 1, pp. 15–23, Jan. 2015.

[8] M. Rubinstein, A. Shamir, and S. Avidan, "Multi-operator media retargeting," *ACM Trans. Graph.*, vol. 28, no. 3, Jul. 2009, Art. no. 23.

[9] Y. S. Wang, C. L. Tai, O. Sorkine, and T. Y. Lee, "Optimized scale-and stretch for image resizing," *ACM Trans. Graph.*, vol. 27, no. 5, 2008, Art. no. 118.

[10] Y. Guo, F. Liu, J. Shi, Z.-H. Zhou, and M. Gleicher, "Image retargeting using mesh parametrization," *IEEE Trans. Multimedia*, vol. 11, no. 5, pp. 856–867, Aug. 2009.

[11] G.-X. Zhang, M.-M. Cheng, S.-M. Hu, and R. R. Martin, "A shape-preserving approach to image resizing," *Comput. Graph. Forum*, vol. 28, no. 7, pp. 1897–1906, 2009.

[12] D. Panozzo, O. Weber, and O. Sorkine, "Robust image retargeting via axis-aligned deformation," *Comput. Graph. Forum*, vol. 31, pp. 229–236, May 2012.

[13] S.-S. Lin, C.-H. Lin, I.-C. Yeh, S.-H. Chang, C.-K. Yeh, and T.-Y. Lee, "Content-aware video retargeting using object-preserving warping," *IEEE Trans. Vis. Comput. Graph.*, vol. 19, no. 10, pp. 1677–1686, Oct. 2013.

[14] T. D. Basha, Y. Moses, and S. Avidan, "Stereo seam carving a geometrically consistent approach," *IEEE Trans. Pattern Anal. Mach. Intell.*, vol. 35, no. 10, pp. 2513–2525, Oct. 2013.

[15] J. Lei, M. Wu, C. Zhang, F. Wu, N. Ling, and C. Hou, "Depth-preserving stereo image retargeting based on pixel fusion," *IEEE Trans. Multimedia*, vol. 19, no. 7, pp. 1442–1453, Jul. 2017.

[16] B. Li, L.-Y. Duan, C.-W. Lin, T. Huang, and W. Gao, "Depth-preserving warping for stereo image retargeting," *IEEE Trans. Image Process.*, vol. 24, no. 9, pp. 2811–2826, Sep. 2015.

[17] C.-H. Chang, C.-K. Liang, and Y.-Y. Chuang, "Content-aware display adaptation and interactive editing for stereoscopic images," *IEEE Trans. Multimedia*, vol. 13, no. 4, pp. 589–601, Aug. 2011.

[18] W. Yan, C. Hou, B. Wang, and L. Wang, "Content-aware disparity adjustment for different stereo displays," *Multimedia Tools Appl.*, vol. 76, no. 8, pp. 10465–10479, Apr. 2017.

[19] F. Shao, W. Lin, W. Lin, Q. Jiang, and G. Jiang, "QoE-guided warping for stereoscopic image retargeting," *IEEE Trans. Image Process.*, vol. 26, no. 10, pp. 4790–4805, Oct. 2017.

[20] K. Utsugi, T. Shibahara, T. Koike, K. Takahashi, and T. Naemura, "Seam carving for stereo images," in *Proc. 3DTV-Conf., True Vis.-Capture, Transmiss. Display 3D Video (3DTV-CON)*, Jun. 2010, pp. 1–4.

[21] D. Lu, H. Ma, and L. Liu, "Visually preserving stereoscopic image retargeting using depth carving," *J. Electron. Imag.*, vol. 25, no. 2, 2016, Art. no. 023029.

[22] J. Shen, D. Wang, and X. Li, "Depth-aware image seam carving," *IEEE Trans. Cybern.*, vol. 43, no. 5, pp. 1453–1461, Oct. 2013.

[23] B. Yue, C. -P. Hou, and Y. Zhou, "Improved seam carving for stereo image resizing," *EURASIP J. Wireless Commun. Netw.*, vol. 2013, no. 1, 2013, Art. no. 116.

[24] Y. Chen, Y. Pan, M. Song, and M. Wang, "Improved seam carving combining with 3D saliency for image retargeting," *Neurocomputing*, vol. 151, pp. 645–653, Mar. 2015.

[25] F. Shao, W. Lin, W. Lin, G. Jiang, M. Yu, and R. Fu, "Stereoscopic visual attention guided seam carving for stereoscopic image retargeting," *J. Display Technol.*, vol. 12, no. 1, pp. 22–30, Jan. 2016.

[26] K.-C. Lien and M. Turk, "On preserving structure in stereo seam carving," in *Proc. Int. Conf. 3D Vis. (3DV)*, Oct. 2015, pp. 571–579.

[27] S.-S. Lin, C.-H. Lin, Y.-H. Kuo, and T.-Y. Lee, "Consistent volumetric warping using floating boundaries for stereoscopic video retargeting," *IEEE Trans. Circuits Syst. Video Technol.*, vol. 26, no. 5, pp. 801–803, May 2016.

[28] J. W. Yoo, S. Yea, and I. K. Park, "Content-driven retargeting of stereoscopic images," *IEEE Signal Process. Lett.*, vol. 20, no. 5, pp. 519–522, May 2013.

[29] F. Shao, L. Shen, Q. Jiang, R. Fu, and G. Jiang, "StereoEditor: Controllable stereoscopic display by content retargeting," *Opt. Express*, vol. 25, no. 26, pp. 33202–33215, Dec. 2017.

[30] S.-P. Du, S.-M. Hu, and R. R. Martin, "Changing perspective in stereoscopic images," *IEEE Trans. Vis. Comput. Graphics*, vol. 19, no. 8, pp. 1288–1297, Aug. 2013.

[31] R. F. Tong, Y. Zhang, and K. L. Cheng, "StereoPasting: Interactive composition in stereoscopic images," *IEEE Trans. Vis. Comput. Graphics*, vol. 19, no. 8, pp. 1375–1385, Aug. 2013.

[32] S.-J. Luo, Y.-T. Sun, I.-C. Shen, B.-Y. Chen, and Y.-Y. Chuang, "Geometrically consistent stereoscopic image editing using patch-based synthesis," *IEEE Trans. Vis. Comput. Graphics*, vol. 21, no. 1, pp. 56–67, Jan. 2015.

[33] M. Lang, A. Hornung, O. Wang, S. Poulakos, A. Smolic, and M. Gross, "Nonlinear disparity mapping for stereoscopic 3D," *ACM Trans. Graph.*, vol. 29, no. 4, 2010, Art. no. 75.

[34] T. Yan, R. W. Lau, Y. Xu, and L. Huang, "Depth mapping for stereoscopic videos," *Int. J. Comput. Vis.*, vol. 102, nos. 1–3, pp. 293–307, 2013.

[35] M. Wang, X.-J. Zhang, J. Liang, S. Zhang, and R. R. Martin, "Comfort-driven disparity adjustment for stereoscopic video," *Comput. Vis. Media*, vol. 2, no. 1, pp. 3–17, Mar. 2016.

[36] J. Lei *et al.*, "Shape-preserving object depth control for stereoscopic images," *IEEE Trans. Circuits Syst. Video Technol.*, vol. 28, no. 12, pp. 3333–3344, Dec. 2018.

[37] C. Oh, B. Ham, S. Choi, and K. Sohn, "Visual fatigue relaxation for stereoscopic video via nonlinear disparity remapping," *IEEE Trans. Broadcast.*, vol. 61, no. 2, pp. 142–153, Jun. 2015.

[38] F. Shao, W. Lin, Z. Li, G. Jiang, and Q. Dai, "Toward simultaneous visual comfort and depth sensation optimization for stereoscopic 3-D experience," *IEEE Trans. Cybern.*, vol. 47, no. 12, pp. 4521–4533, Dec. 2017.

[39] F. Shao, W. Lin, G. Jiang, and Q. Dai, "Models of monocular and binocular visual perception in quality assessment of stereoscopic images," *IEEE Trans. Comput. Imag.*, vol. 2, no. 2, pp. 123–135, Jun. 2016.

[40] D. Sun, S. Roth, and M. J. Black, "Secrets of optical flow estimation and their principles," in *Proc. Int. Conf. Comput. Vis. Pattern Recognit. (CVPR)*, Jun. 2010, pp. 2432–2439.

[41] M. Lambooij, M. Fortuin, I. Heynderickx, and W. Ijsselsteijn, "Visual discomfort and visual fatigue of stereoscopic displays: A review," *J. Imag. Sci. Technol.*, vol. 53, no. 3, 2009, Art. no. 0302011.

[42] F. Shao, W. Lin, R. Fu, M. Yu, and G. Jiang, "Optimizing multiview video plus depth retargeting technique for stereoscopic 3D displays," *Opt. Express*, vol. 25, no. 11, pp. 12478–12492, May 2017.

[43] I. Tsirlin, L. M. Wilcox, and R. S. Allison, "A computational theory of da Vinci stereopsis," *J. Vis.*, vol. 14, no. 7, pp. 1–26, 2014.
[44] Q. Jiang, F. Shao, G. Jiang, M. Yu, Z. Peng, and C. Yu, "A depth perception and visual comfort guided computational model for stereoscopic 3D visual saliency," *Signal Process., Image Commun.*, vol. 38, pp. 57–69, Oct. 2015.
[45] T.-C. Yen, C.-M. Tsai, and C.-W. Lin, "Maintaining temporal coherence in video retargeting using mosaic-guided scaling," *IEEE Trans. Image Process.*, vol. 20, no. 8, pp. 2339–2351, Aug. 2011.
[46] Q. Jiang, F. Shao, G. Jiang, M. Yu, and Z. Peng, "Three-dimensional visual comfort assessment via preference learning," *J. Electron. Imag.*, vol. 24, no. 4, Jul. 2015, Art. no. 043002.
[47] H. Sohn and Y. J. Jung. (2012). *IVY Lab Stereoscopic Image Database*. [Online]. Available: http://www.ivylab.kaist.ac.kr/demo/3DVCA/3DVCA.htm
[48] D. Scharstein, R. Szeliski, and C. Pal. (2012). *Middlebury Stereo Datasets*. [Online]. Available: http://vision.middlebury.edu/stereo/data
[49] *Subjective Video Quality Assessment Methods for Multimedia Applications*, document Rec. ITU-T P.910, ITU Telecommunication Sector of ITU, 1999.
[50] C.-C. Hsu, C.-W. Lin, Y. Fang, and W. Lin, "Objective quality assessment for image retargeting based on perceptual geometric distortion and information loss," *IEEE J. Sel. Topics Signal Process.*, vol. 8, no. 3, pp. 377–389, Jun. 2014.
[51] Y. Zhang, Y. Fang, W. Lin, X. Zhang, and L. Li, "Backward registration-based aspect ratio similarity for image retargeting quality assessment," *IEEE Trans. Image Process.*, vol. 25, no. 9, pp. 4286–4297, Sep. 2016.
[52] L. Zhang, K. Li, Z. Ou, and F. Wang, "Seam warping: A new approach for image retargeting for small displays," *Soft Comput.*, vol. 21, no. 2, pp. 447–457, 2017.

XIONGLI CHAI received the B.S. degree from Ningbo University, Ningbo, China, in 2017, where he is currently pursuing the M.S. degree. His current research interests include image/video processing and quality assessment.

FENG SHAO (M'16) received the B.S. and Ph.D. degrees in electronic science and technology from Zhejiang University, Hangzhou, China, in 2002 and 2007, respectively. He was a Visiting Fellow with the School of Computer Engineering, Nanyang Technological University, Singapore, in 2012. He is currently a Professor with the Faculty of Information Science and Engineering, Ningbo University, China. He has published over 100 technical articles in refereed journals and proceedings in the areas of 3D video coding, 3D quality assessment, and image perception. He has received the Excellent Young Scholar Award from NSF of China, in 2016.

QIUPING JIANG (S'17) received the Ph.D. degree from Ningbo University, in 2018. From 2017 to 2018, he was a Visiting Student with the School of Computer Science and Engineering, Nanyang Technological University, Singapore. He is currently an Associate Professor with the School of Information Science and Engineering, Ningbo University, Ningbo, China. His research interests include image processing, visual perception modeling, and computer vision. He was a recipient of the 2017 JVCI Best Paper Award Honorable Mention as the first author. He is a Reviewer of several prestigious journals and conferences such as the IEEE TNNLS, IEEE TIP, IEEE TCSVT, IEEE TMM, IEEE TSIPN, ICME, and ICIP.

YO-SUNG HO (SM'06–F'16) received the B.S. and M.S. degrees in electronic engineering from Seoul National University, Seoul, South Korea, in 1981 and 1983, respectively, and the Ph.D. degree in electrical and computer engineering from the University of California at Santa Barbara, Santa Barbara, in 1990. He joined the Electronics and Telecommunications Research Institute (ETRI), Daejon, South Korea, in 1983. From 1990 to 1993, he was with Philips Laboratories, Briarcliff Manor, NY, USA, where he was involved in the development of the advanced digital high-definition television system. In 1993, he rejoined as the Technical Staff of the ETRI, where he was involved in the development of the Korean DBS digital television and high-definition television systems. Since 1995, he has been with the Gwangju Institute of Science and Technology, Gwangju, South Korea, where he is currently a Professor with the Information and Communications Department. His research interests include digital image and video coding, image analysis and image restoration, advanced video coding techniques, digital video and audio broadcasting, three-dimensional video processing, and content-based signal representation and processing.